frontiers in NEUROLOGY

ORIGINAL RESEARCH ARTICLE
published: 04 April 2011
doi: 10.3389/fneur.2011.00019

Low level primary blast injury in rodent brain

Pamela B. L. Pun[1], Enci Mary Kan[1], Agus Salim[2], Zhaohui Li[3], Kian Chye Ng[1], Shabbir M. Moochhala[1], Eng-Ang Ling[4], Mui Hong Tan[1] and Jia Lu[1]*

[1] Combat Care Laboratory, Defence Medical and Environmental Research Institute, DSO National Laboratories, Singapore
[2] Department of Epidemiology and Public Health, Yong Loo Lin School of Medicine, National University of Singapore, Singapore
[3] Bek Chai Heah Laboratory of Cancer Genomics, Cellular and Molecular Research, Humphrey Oei Institute of Cancer Research, National Cancer Centre, Singapore
[4] Department of Anatomy, Yong Loo Lin School of Medicine, National University of Singapore, Singapore

Edited by:
Marten Risling, Karolinska Institutet, Sweden

Reviewed by:
Hans Lindå, Karolinska Institutet, Sweden
Ibolja Cernak, Johns Hopkins University, USA

***Correspondence:**
Jia Lu, Combat Care Laboratory, Defence Medical and Environmental Research Institute, DSO National Laboratories, 27 Medical Drive, Singapore 117510, Singapore.
e-mail: ljia@dso.org.sg

The incidence of blast attacks and resulting traumatic brain injuries has been on the rise in recent years. Primary blast is one of the mechanisms in which the blast wave can cause injury to the brain. The aim of this study was to investigate the effects of a single sub-lethal blast over pressure (BOP) exposure of either 48.9 kPa (7.1 psi) or 77.3 kPa (11.3 psi) to rodents in an open-field setting. Brain tissue from these rats was harvested for microarray and histopathological analyses. Gross histopathology of the brains showed that cortical neurons were "darkened" and shrunken with narrowed vasculature in the cerebral cortex day 1 after blast with signs of recovery at day 4 and day 7 after blast. TUNEL-positive cells were predominant in the white matter of the brain at day 1 after blast and double-labeling of brain tissue showed that these DNA-damaged cells were both oligodendrocytes and astrocytes but were mainly not apoptotic due to the low caspase-3 immunopositivity. There was also an increase in amyloid precursor protein immunoreactive cells in the white matter which suggests acute axonal damage. In contrast, Iba-1 staining for macrophages or microglia was not different from control post-blast. Blast exposure altered the expression of over 5786 genes in the brain which occurred mostly at day 1 and day 4 post-blast. These genes were narrowed down to 10 overlapping genes after time-course evaluation and functional analyses. These genes pointed toward signs of repair at day 4 and day 7 post-blast. Our findings suggest that the BOP levels in the study resulted in mild cellular injury to the brain as evidenced by acute neuronal, cerebrovascular, and white matter perturbations that showed signs of resolution. It is unclear whether these perturbations exist at a milder level or normalize completely and will need more investigation. Specific changes in gene expression may be further evaluated to understand the mechanism of blast-induced neurotrauma.

Keywords: primary blast injury, central nervous system, histopathology, immunohistochemistry, gene expression

INTRODUCTION

Blast attacks involving weapons such as roadside bombs, grenades, and improvised explosive devices (IEDs) are an increasingly common feature of terrorist attacks, with as many as 1513 such attacks recorded in the period of January to November 2007, affecting both civilian and military populations and resulting in over 16,000 casualties (Lawson Terrorism Information Centre, 2009). In particular, blast-induced neurotrauma (BINT) is an increasing problem for which mild traumatic brain injury (MTBI) forms the majority of these injuries (Ling et al., 2009; Cernak and Noble-Haeusslein, 2010). Despite the pressing urgency for accurate and effective diagnostic, prognostic, and therapeutic approaches to blast injuries, there remain significant gaps in our knowledge of this condition (Kochanek et al., 2009).

Primary neurotrauma occurs when the insult delivers a direct blow to the head which may be penetrating or non-penetrating (closed head). In a blast injury, primary injury is a result of the directs effects of the blast wave to the head compared to other forms of blast injuries such as secondary (e.g., victim is hit on head by an object propelled by the blast wave) and tertiary (e.g., victim is flung by the blast wave against an object and injures his head) injuries. The most commonly assessed blast wave parameter for primary blast injury is usually the peak blast over pressure (BOP), duration of the positive phase and impulse. The effects of primary blast injury on air-containing organs such as the lungs have been widely investigated and characterized (Kirkman and Watts, 2011). Blast-induced pulmonary injury thresholds have also been elucidated and refined (Bowen et al., 1968; Rafaels et al., 2010). Advancement in body armor material and protection has been able to mitigate in part, the vulnerability of pulmonary injuries to blast (Phillips et al., 1988) though not totally. Together with improved efficiencies in medical evacuations and advances in medical care which contribute to increased survival rate, incidences of BINT are on the rise in modern warfare.

Given the prevalence of BINT, the mechanism of primary blast injury to the central nervous system (CNS) is less well characterized and especially so for blast-induced MTBI. To date, most primary blast injury rodent CNS research has focused on peak BOPs > 110 kPa. However, it has been reported that BOPs > 110 kPa can also cause concomitant pulmonary injury

in animals with high incidence of mortality (Bauman et al., 1997; Gorbunov et al., 2004; Chavko et al., 2006; Long et al., 2009). Hence, we were particularly interested in the effects of low-intensity blast on the brain at peak BOPS < 110 kPa without causing overt pulmonary damage and mortality.

Previous studies investigating BINT in rodents have reported a wide spectrum of perturbations post-blast that encompass cerebrovascular changes, white matter damage, neuronal changes in the hippocampus, oxidative stress, and increased blood–brain barrier permeability (Bauman et al., 1997; Cernak et al., 2001a,b; Long et al., 2009; Cernak, 2010; Readnower et al., 2010; Risling et al., 2011). Recent literature has also pointed toward the presence of cerebral inflammation that could be mediated by systemic inflammation due to the CNS effects of the primary blast wave through the unprotected torso (Cernak, 2010). Hence, in this low level blast study, we aimed to profile the acute changes post-blast especially with regards to regions vulnerable to apoptotic cell death and inflammation through the activation of microglial cells which are the major inflammatory cells in the CNS.

Furthermore, we also sought to profile changes in gene expression post-blast for the identification of broad functional changes through clustering and to provide a platform for biomarker discovery. Biomarkers should be definitive indicators of pathogenic processes (Biomarkers Definitions Working Group, 2001) which are sorely lacking for MTBI for which better experimental designs into underlying molecular mechanisms are required (Svetlov et al., 2009). A proteomics approach to identifying relevant molecules has previously been suggested (Agoston et al., 2009). We present here, a microarray technique that can be applied to low level primary blast research and also venture to provide a conceptual model of an alternative and complementary genomics-based approach.

MATERIALS AND METHODS

ANIMALS AND BLAST EXPOSURE

Animal experiments were approved by the DSO Institutional Animal Care and Use Committee (DSO IACUC). Male Sprague-Dawley rats (250–350 g) were used for this study. Rats were anesthetized prior to blast exposure with an intraperitoneal injection of 75 mg/kg ketamine and 10 mg/kg xylazine. The animals were then secured with Velcro straps in metal cages that were anchored to the ground at the blast site. The source of BOP was 120 kg of 2,4,6-trinitrotoluene (TNT). Blast sensors (seven side-on pressure gages and three stagnation pressure gages) were used to monitor intensity and duration of BOP exposure during test and actual blast trials. Animals were placed at either 24 or 30 m away from the TNT source and were exposed to different sub-lethal BOP intensities (i.e., low, high). Six to eight animals were strapped loosely using Velcro to a metal mesh cage at the specified distances and doused with water to minimize dehydration and singeing of fur. A 0.4 m × 0.4 m concrete block was placed between the animals and the explosive source at a distance of 1.5 m from the animals. This block served as a shield against debris from the explosion, thus protecting animals against secondary blast injuries due to the projectiles. A schematic of the blast set-up is given in **Figure 1A**. Preliminary trials and simulations revealed no influence of the block on the blast wave at the position of the animals (data not shown). Control animals were transported to the blast

A

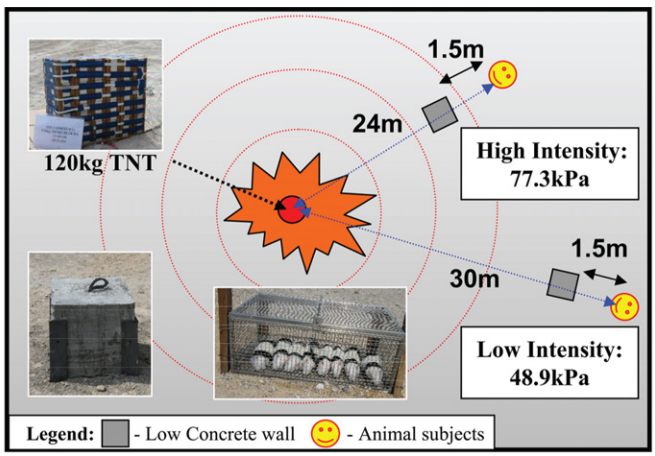

B

Blast condition	Distance (m)	Peak blast over pressure (kPa)	Positive duration (msec)	Mortality (%)
Low	30	48.9	14.5	4.4
High	24	77.3	18.2	8.3

FIGURE 1 | (A) Schematic of blast set-up for six to eight rodents placed in a mesh metal cage at 24 m (high intensity) and 30 m (low intensity) from blast source (120 kg TNT) shielded from debris with a concrete block (0.4 m × 0.4 m) at 1.5 m from the animals. **(B)** Actual blast parameters: pressure (kPa) and duration (milliseconds) and mortality (%) at low and high blast exposure.

site then anesthetized as with the blast-exposed animals, but were not exposed to the actual blast. After blast exposure, the animals were returned to the animal holding facility and allowed to recover from the effects of anesthesia. Access to food and drinks was *ad libitum*. The animals were sacrificed at day 1, day 4, and day 7 after the blast.

HISTOPATHOLOGY AND IMMUNOHISTOCHEMISTRY

By method of transcardial perfusion, the animals were perfused with Ringer's solution until the liver and lungs were cleared of blood followed by 10% buffered paraformaldehyde. The brains were harvested and post-fixed in 10% buffered formalin. The brains were then dehydrated in an ascending series of alcohol, cleared with xylene, and then embedded in paraffin wax. Paraffin sections of 4 μm thickness were then cut and microwaved in citrate buffer for antigen retrieval and blocked with peroxidase blocking reagent (S2023, DAKO UK Ltd, UK). Brain and lung sections were stained for routine histology using hematoxylin and eosin (H&E) for general morphology analysis. For apoptosis staining, brain sections were stained according to the protocol provided in the ApopTag® Peroxidase *In Situ* Apoptosis Detection Kit (S7100, Chemicon International, Inc., MA, USA). For the preparation of double-labeled brain sections, a second antibody of rabbit anti-glial fibrillary acidic protein (GFAP) (AB5804, Chemicon International, Inc., MA, USA) diluted 1:1500 in PBS, biotinylated *Ricinus communis* Agglutinin I (RCA_{120}) anti-lectin (B-1085, Vector Laboratories, Inc., CA, USA) diluted 1:1000 in PBS or rabbit polyclonal anti-myelin basic protein (MBP; AB980, Chemicon International, Inc., MA, USA) diluted 1:200 in PBS was used to detect GFAP, lectin, and MBP respectively. For immunohistochemistry, brain sections were also incubated with rabbit polyclonal anti-caspase-3 (#RB-1197-P, Thermo Fisher Scientific Inc., USA) diluted 1:100 in PBS; rabbit anti-ionized calcium binding adaptor molecule-1 (Iba-1; #019-19741, Wako Pure Chemical) diluted 1:500 in PBS; and rabbit polyclonal amyloid β precursor protein (APP; AB17467, Abcam) diluted 1:100 in PBS; for detection of caspase-3, Iba-1, and APP respectively. Subsequent antibody detection was carried out using either anti-mouse or anti-rabbit IgG (Envision + system-HRP, DAKO UK Ltd, UK) except for lectin which was carried out using horseradish peroxidase streptavidin (SA-5004, Vector Laboratories). All samples were then visualized using 3,3′-diaminobenzidine (DAB) and examined under a light microscope (Olympus, Japan). A cell count of at least three sections at 20× magnification of TUNEL, Iba-1, and APP positive cells in the white matter was carried out and results are expressed as mean ± standard error of the mean (SEM). Statistical comparison between groups was performed by one-way ANOVA with *post hoc* Tukey's HSD test. Significance was accepted at $p < 0.05$.

MICROARRAY

Brain tissue from animals exposed to the lower BOP were harvested, quick frozen in lqN_2 and stored at −80°C for subsequent microarray analyses. RNA was isolated using standard Trizol-based RNA extraction methods. The RNA quality was then determined based on RNA integrity number (RIN) and an electropherogram, both of which were analyzed using the Agilent 2100 Bioanalyzer platform (Agilent Technologies). Only samples with RIN greater than 6 were used (Fleige and Pfaffl, 2006). RNA samples were amplified and labeled with Cy3, hybridized to Agilent Whole Rat Genome Oligo Microarrays 4x44k, and analyzed using a microarray scanner system. All procedures were carried out in duplicates using commercial kits (Agilent Technologies) by a microarray service provider (Miltenyi Biotec GmbH, Germany). Microarray results were analyzed using R/Bioconductor and Partek Genomic Suite (Partek, MO, USA). Two independent analyses were conducted. The first set of analysis compared the expression levels of genes in blast-exposed animals vs. that in controls at each time-point. The second set of analysis investigated the changes in log ratio of blast-exposed vs. control animals [log (blast/control)] over time [e.g., log $(\text{blast/control})_{\text{day 4}}$ vs. log $(\text{blast/control})_{\text{day 1}}$, log $(\text{blast/control})_{\text{day 7}}$ vs. log $(\text{blast/control})_{\text{day 1}}$]. The overall type I error was taken at 0.01, and *p*-values were corrected for multiple testings using false discovery rates.

RESULTS

BLAST EXPOSURE AND SURVIVAL

A total of 58 animals were used in this study, of which 11 were controls, 23 were exposed to BOP at 48.9 kPa (or 7.1 psi) and positive over pressure duration of 14.5 ms at 30 m from TNT source, and 24 were exposed to BOP at 77.3 kPa (or 11.3 psi) and positive over pressure duration of 18.2 ms at 24 m (**Figure 1B**). For the purposes of the current work, we shall refer to the blast exposure conditions employed in simplistic terms as either high (BOP = 77.3 kPa) or low (BOP = 48.9 kPa) intensity. Corresponding mortality rates for the groups (low, high) were 4.4 and 8.3% respectively (**Figure 1B**). All of these animals died within 30 min of blast exposure. Deaths in the blast groups revealed pulmonary hemorrhage post-mortem. Surviving rats were used for subsequent investigation.

HISTOLOGY AND IMMUNOHISTOCHEMISTRY OF BLAST INJURIES

Lung gross histopathology

Rats were sacrificed at day 1, day 4, or day 7 after blast for investigation. Two tissues were examined, namely the brain and lungs. Other tissues were not examined as no external hemorrhage was observed. There was no apparent lung injury in both blast-exposed groups on day 1 post-blast. However, a few petechiae and ecchymoses were observed in the periphery of lung tissue upon harvesting at day 4 and day 7 after blast. H&E staining of the lung sections revealed alveolar lesions with accumulation of red blood corpuscles in lung alveolar space at day 4 and day 7 post high-intensity blast (**Figure 2**).

Brain and lung gross histopathology

No obvious extra- and/or sub-dural hemorrhage was observed in the brains of all blast-exposed animals relative to the untreated controls H&E staining of brain sections from cerebral cortex showed darkened neurons (identified from the presence of projecting dendrites and polygonal shape of cell body) after high-intensity blast mostly at day 1 post-blast which appeared to abate at day 4 and day 7. These darkened neurons were also shrunken as evidenced by the presence of peri-somal spaces. Furthermore, the vasculature appeared to be narrowed at day 1 and day 4 post-blast compared to control (**Figure 3**).

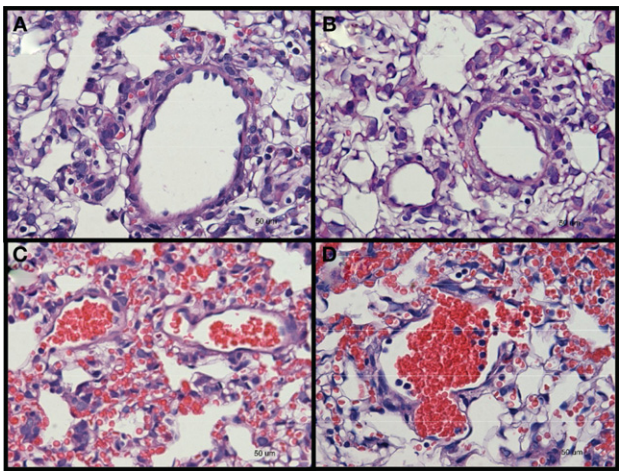

FIGURE 2 | Hematoxylin and eosin stained sections of lung tissues from (A) control, and low-intensity blast-exposed animals at (B) day 1 (C) day 4, and (D) day 7, after blast signs of hemorrhage, macrophage infiltration, and thickening of the alveolar septae, were observed at day 4 and day 7 after blast injury.

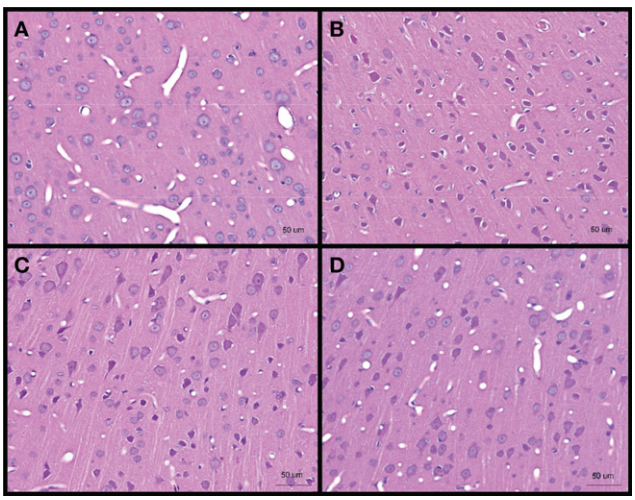

FIGURE 3 | Hematoxylin and eosin stained sections of brain cerebral cortex from (A) control, and low-intensity blast-exposed animals at (B) day 1 (C) day 4, and (D) day 7 after blast. Darkened and shrunken neurons evidenced by the presence of peri-somal spaces at day 1 post-blast compared to control and in lesser quantities at day 4 and day 7 post-blast. Vasculature appears to be narrowed in day 1 and day 4 post-blast compared to control.

White matter damage

To confirm the presence of injury in the brains of rats exposed to high- and low-intensity BOP, TUNEL and caspase-3 staining was carried out to identify apoptotic cells in the brains. There were only a few cells positive for caspase-3 (not shown) compared to TUNEL-positive cells in the white matter. There was significantly more TUNEL-positive cells in the white matter of blast-exposed rats at high- and low-intensity relative to control on day 1 after blast (**Figure 4**). By day 7, however, there appeared to be no major difference between controls and blast-treated rats (data not shown). Double-staining for TUNEL and non-neuronal cells (GFAP, lectin, or MBP) revealed that the cells with DNA fragmentation were mainly oligodendrocytes and astrocytes, but not microglial cells (**Figure 5**). Iba-1 staining for CNS macrophages/microglia also showed no changes in microglia density between control and both blast-groups at day 1 post-blast (**Figure 6**). In addition to the presence of apoptotic astrocytes and oligodendrocytes, APP immunostaining was also significantly increased in both blast conditions compared to control on day 1 after blast (**Figure 7**).

GENE EXPRESSION CHANGES IN MILD TRAUMATIC BRAIN INJURY

Microarray analyses of brain RNA samples from both control and rats exposed to low-intensity blast was carried out to determine gene expression changes. For the purpose of analysis, we hypothesized that functionally relevant genes are likely to include those whose expressions are significantly altered by blast exposure and/or show a significant time evolution after blast.

In our first set of analyses, we found 5786 probe sets which showed significant changes in the blast-exposed group relative to the controls at least one time-point. Most of these probe sets either had no confirmed identities or no known biological functions. Only 676 were established genes with well-defined functions (**Table A1** in Appendix). We grouped these genes according to their functions and the results are shown in **Figure 8**. It appears that most changes took place at day 1 and day 4 after blast, with far fewer alterations observed at day 7. Clustering of the genes whose expressions varied most between arrays revealed high concordance between two replicates under the same condition which cluster together. In particular, day 1 and day 7 replicates clusters seemed similar while day 4 is different (**Figure 9**).

Our second set of analyses revealed 203 probe sets that showed significant time-course evolution, i.e., the log $(\text{blast/control})_{\text{day 4 or day 7}}$ was different relative to that at day 1. Based upon their time-evolution pattern, these 203 probe sets were grouped into eight clusters based on similar evolution (**Figure 10**). The biological functions of genes in each cluster, except clusters 5 and 8 which do not have genes with information, are given in **Table A2** of Appendix. Out of the 203, only 34 are known genes with established functions (**Table 1**). Between our two sets of microarray analyses, there was an overlap of 10 genes (**Table 2**).

DISCUSSION

Blast-induced neurotrauma is the signature of the modern war (Elder et al., 2010). We were particularly interested in mild TBI as it accounts for over 77.8% of all TBI injuries sustained during combat (Defense and Veterans Brain Injury Center, 2010). In our open field blast test, we set out to investigate the effects of two relatively low BOP exposures of 77.3 and 48.9 kPa to cause mild BINT and to determine its effects on pulmonary injury in rodents with no body armor. The low BOP exposure was determined from the Bowen's curve to determine if these BOP values could cause mild BINT without any overt pulmonary damage and also to minimize mortality in the animals. At the time of our study, there was only one report investigating the effects of peak BOP < 100 kPa on the effects in the rodent CNS (Saljo et al., 2009).

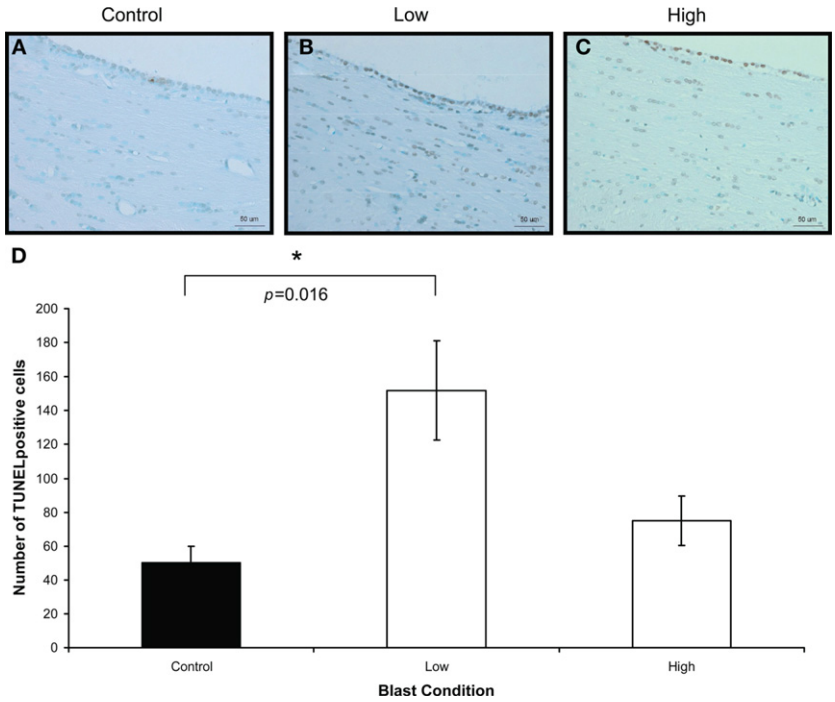

FIGURE 4 | Iba-1 immunostaining (brown) of (A) control (B) low, and (C) high, blast exposure 1 day after blast. Scale bar = 50 μm. **(D)** Mean number of Iba-1 positive cells per field view in the corpus callosum of control, low ($p = 0.26$ vs. control) and high ($p = 0.019$ vs. control) blast-exposed animals 1 day after blast at ×20 magnification. No difference in Iba-1 positive cells was found between blast exposure groups (low and high) and control. *$p < 0.05$.

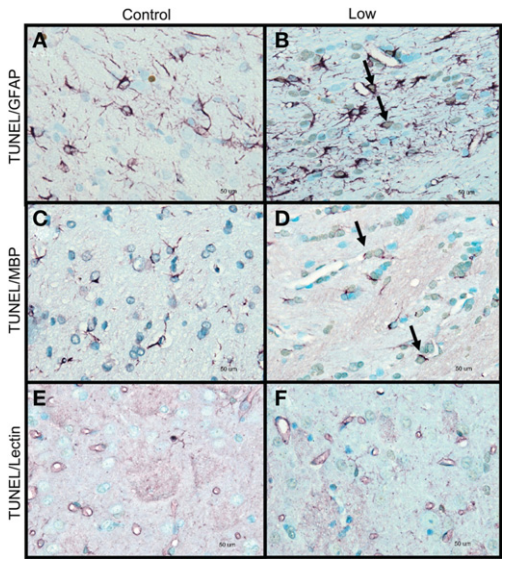

FIGURE 5 | Double-labeling of non-neuronal cells with TUNEL for apoptotic cells (light brown staining, indicated by small arrows) and glia markers (purple staining) for (A,B) apoptotic astrocytes, indicated by thick arrows (TUNEL and GFAP double-labeling). (C,D) Apoptotic oligodendrocytes, indicated by thick arrows (TUNEL and MBP double-labeling). **(E,F)** Lectin-positive microglia and TUNEL-labeled cells (TUNEL and lectin double-labeling). Control animals **(A,C,E)**, low-intensity blast-exposed animals **(B,D,F)**. Note lack of overlapping of labeling in apoptotic cells and microglia in low-intensity blast-exposed animals. Scale bar = 50 μm.

Our findings showed the appearance of hemorrhagic lesions in the lung which is a feature of pulmonary blast injury even at the test levels of BOP of 77.3 and 48.9 kPa compared to previous studies in which lung injury was reported at higher BOP exposure of 118 kPa (Chavko et al., 2006; Gorbunov et al., 2006). The late appearance of lung petechiae and alveolar hemorrhage at day 4 and day 7 after blast suggests a delayed response as opposed to immediate (as early as 2 h) pulmonary injury that could occur at higher BOPs (Gorbunov et al., 2006). Recent evidence investigating a BOP model <110 kPa also demonstrated that a shockwave of 11.5 kPa resulted in no evidence of lung injury but was evident at 66 kPa (Park et al., 2010). Hence, it may be suggested that the BOP range of 48.9–77.3 kPa represents the threshold for blast-induced lung injury in the unprotected rodent. The use of improved protective body armor in combat situations has largely mitigated against pulmonary injury and mortality (Phillips et al., 1988). It is now generally accepted that the threshold for BINT is higher than that of pulmonary injury. Pulmonary blast injury has been reported to be due to the pressure changes at the tissue-density interface (DePalma et al., 2005). The Bowen's curve for which the study's sub-lethal BOP levels were chosen was based on this theory. However, other factors such as the viscoelasticity of the tissue (Stuhmiller, 1997) and internal spalling and implosion (Treadwell, 1989) may also contribute to pulmonary blast injury.

The BOP exposure to animals in our study resulted in the "darkening" or enhanced H&E staining of cortical neurons in the gray matter which may be due to the condensation of the neuronal cytoplasm which has also been previously reported to occur in a global cerebral ischemic condition (Kawai et al., 1992). These

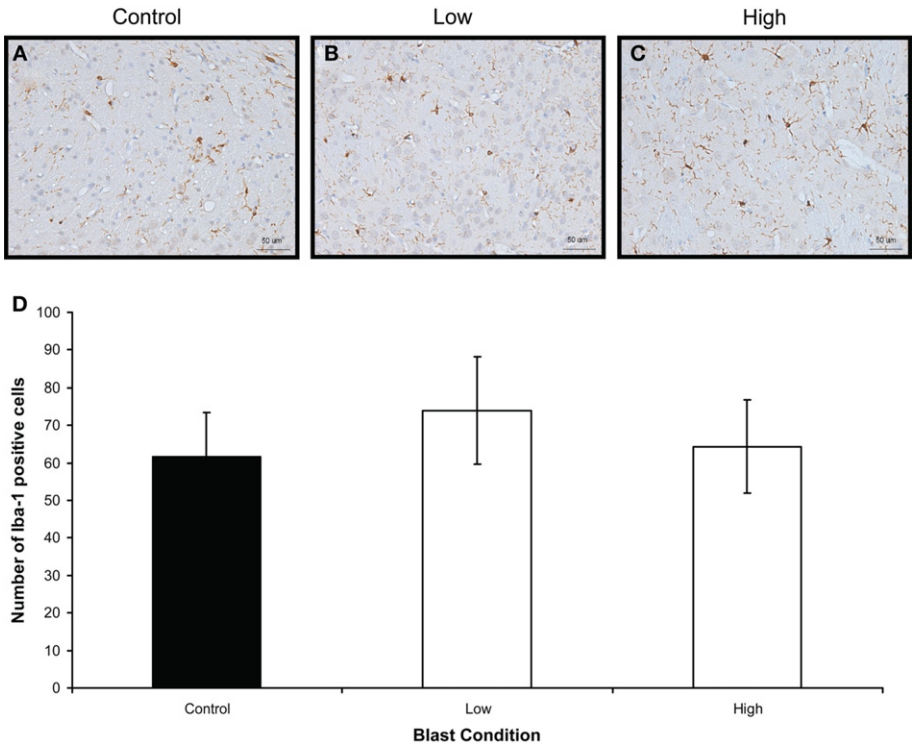

FIGURE 6 | Iba-1 immunostaining (brown) of (A) control (B) low, and (C) high, blast exposure 1 day after blast. Scale bar = 50 μm. **(D)** Mean number of Iba-1 positive cells per field view in the corpus callosum of control, low ($p = 0.26$ vs. control), and high ($p = 0.019$ vs. control) blast-exposed animals 1 day after blast at ×20 magnification. No difference in Iba-1 positive cells was found between blast exposure groups (low and high) and control. *$p < 0.05$.

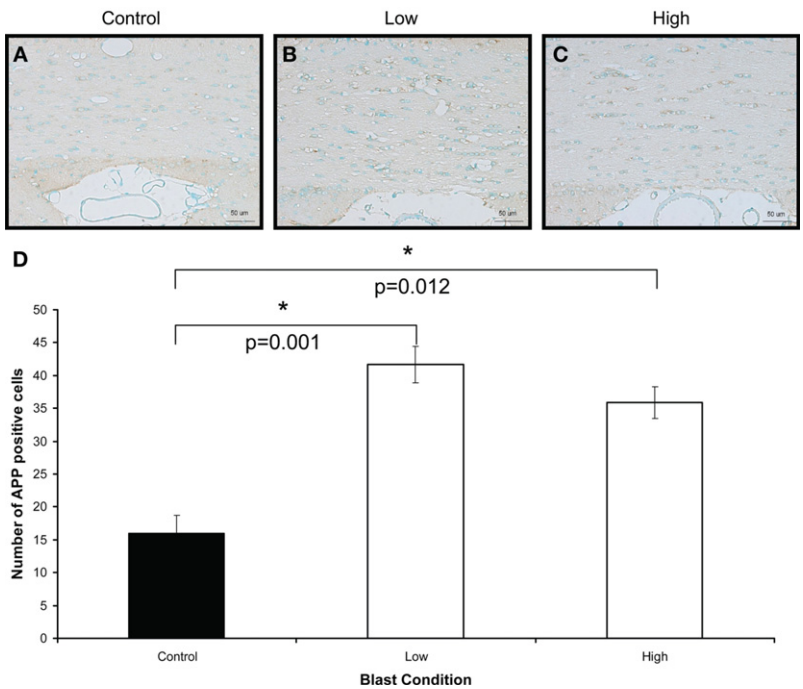

FIGURE 7 | Amyloid β precursor protein immunostaining (brown) of (A) control (B) low, and (C) high, blast exposure 1 day after blast. Scale bar = 50 μm. **(D)** Mean number of APP positive cells per field view in the white matter of control, low ($p = 0.26$ vs. control) and high ($p = 0.019$ vs. control) blast-exposed animals 1 day after blast at ×20 magnification. Both low and high blast exposure animals had significantly higher APP+ cells than control. *$p < 0.05$.

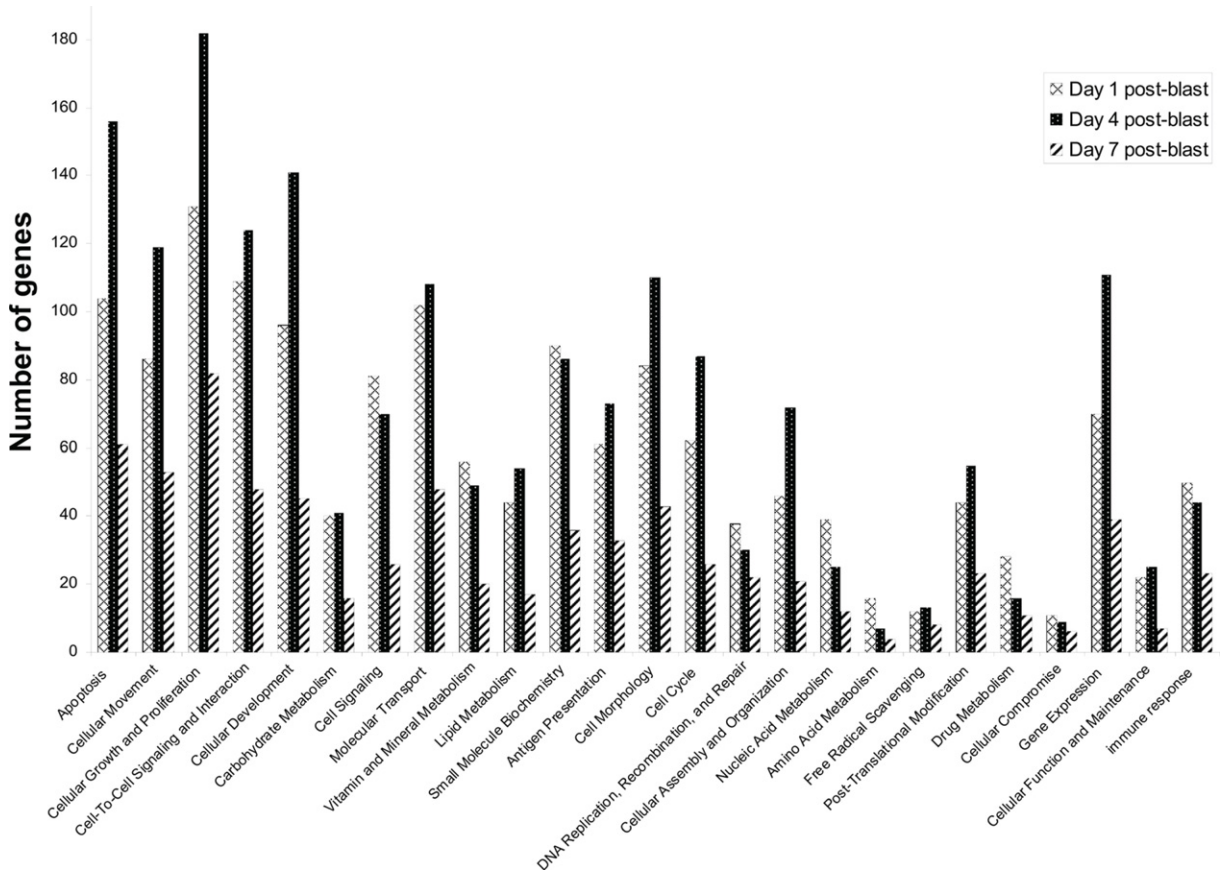

FIGURE 8 | Functional categorization of genes whose expression levels are altered by blast. Genes were categorized based on their biological functions. Probe sets with unknown functions were ignored in this analysis. A total of 1200 functionally characterized genes were identified in our microarray experiments using brain tissue from rats exposed to a BOP of 48.9 kPa. As each gene can have multiple functions, every gene may contribute more than once to the gene count shown here.

cortical changes is also consistent with our previous study investigating BOP of 20 kPa in rodents 1 day post-blast (Moochhala et al., 2004). Furthermore, the changes in vascular profiles post-blast suggest the occurrence of vasospasm which has also been reported as a feature of blast injury (Armonda et al., 2006). The alleviation in darkening at day 4 and day 7 post-blast and a rescue in vascular morphology at day 7 points to the existence of an acute transient ischemic cerebral environment that can recover with time after blast. Interestingly, cerebrovascular changes such as microvascular density and vasospasm have also been reported in studies in blast and impact TBI (Armonda et al., 2006; Park et al., 2010; Svetlov et al., 2010). However, it is unclear whether there is a complete recovery to the original state and whether the mild changes persist. Despite these cortical histopathological changes, TUNEL-staining was not observed in the white matter. This suggests that cortical gray matter and vasculature is affected by the blast wave in a differential manner from white matter.

Our study also showed that low BOP exposures at $<$110 kPa predominantly caused DNA fragmentation in the glial cells of the white matter with corresponding accumulation of APP probably due to axonal damage which is apparent at day 1 post-blast. The presence of white matter damage post-blast is becoming well-documented and the presence of this damage at low BOP levels suggest that primary injury from the shockwave can act to disrupt axonal transport and to cause cell death in oligodendrocytes and astrocytes which play important supportive functions in the white matter. This axonal pathology is further corroborated by findings of early increases in α-II spectrin, an axonal cytoskeletal protein, and sustained expression of NF200, an axonal neurofilament, in a mild BINT rodent model (Park et al., 2010).

Our study was only focused on the head-on exposure of the shockwave to the skull of the animal although it has been suggested that different orientations of the animal can have different pressure transmission, whether direct or reflected off the skull (Chavko et al., 2011), and the effects of different wave propagation on the CNS due to orientation remains to be investigated. Despite reports of blood–brain barrier permeability changes and inflammation post-blast (Bauman et al., 1997; Cernak et al., 2001a,b; Long et al., 2009; Cernak, 2010; Readnower et al., 2010; Risling et al., 2011), we did not find any changes in AQP-4 expression on S100B+ astrocytes (results not shown) as well as changes in Iba-1 immunoreactivity for microglia, the main inflammatory macrophages in the CNS, as well as systemic cytokines (results not shown). These negative findings may be explained by the lower

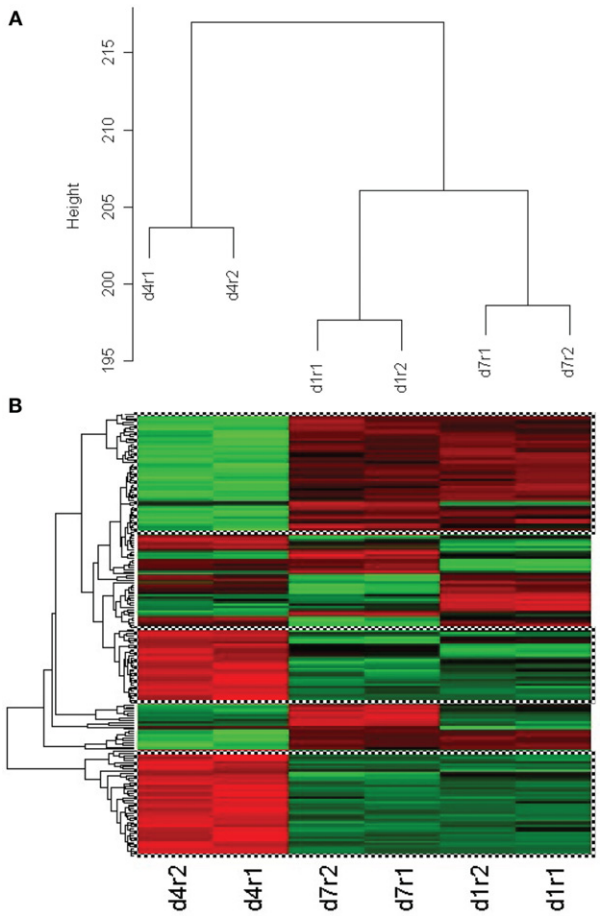

FIGURE 9 | (A) Cluster dendrogram of genes whose expression varied most from control between arrays for two replicates (r1, r2) of the same condition at day 4, day 1, and day 7 after low-intensity blast. Replicates are observed to cluster at the same level whilst clusters for day 4 appear different from day 1 and day 7. **(B)** Clustering of 203 genes that show similar behavior between replicates of day 4 (column 1), day 7 (column 2), and day 1 (column 3) after light intensity blast. Green color represents upregulation whilst red color represents downregulation from control. The topmost cluster (checked box) shows genes that are up-regulated at day 4 but down-regulated at day 1 and day 7, whilst the middle and bottom clusters (checked box) show the opposite trend.

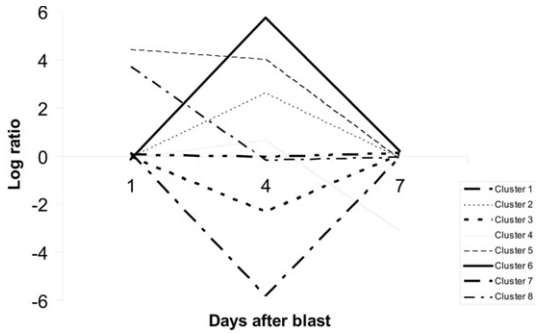

FIGURE 10 | Clustering of probe sets with significant time-course evolution. A total of 203 probe sets showing such evolution were identified, and grouped into eight clusters based on their time-evolution profiles. Probe sets in cluster 1 showed no major variation over time. They are consistently and weakly up-regulated or down-regulated across all time-points. Those in clusters 2 and 6 were up-regulated while those in clusters 3 and 7 were down-regulated at day 4. Probe sets in clusters 4, 5, and 8 were respectively down-regulated at day 7, up-regulated at day 1 and day 4, and up-regulated at day 1 only.

BOPs used in our study or that the animals were not observed for longer periods of time post-blast.

Given that the lethal threshold is lowest for blast lung injury than other organ systems, no significant mortality was expected in our blast model used here. This was confirmed by our findings (4.4% low BOP, 8.3% high BOP). Although two different BOPs were investigated in this study, both lie on the lower limit of the BOP range tested across many experimental blast studies. This may explain the non-significant differences in mortality, histopathological, and immunohistochemical changes between the low and high BOP. However, the blast set-up employed in this study can be used to establish a blast pressure-dependent mortality or morbidity response curve by placing animals at varying distances from the TNT source and by varying the amount of TNT.

Besides the low BOP, the animals were also exposed to a long positive duration of 14.5 and 18.2 ms in the low and high intensity settings respectively due to the distance that the subjects were placed away from the TNT explosive as opposed to other models of blast injury using compressed air, helium, oxyhydrogen or cyclotrimethylenetrinitramine (Reneer et al., 2011). The duration of the overpressure is thought to be of much significance in causing damage (de Candole, 1967) as the length of this positive duration would also affect the impulse at which the animals are subjected to. This longer positive overpressure duration also reflects the increasing use of thermobaric and other novel explosives in the modern war (Rafaels et al., 2010) and could have different mechanisms from other models investigating short positive overpressure durations (Cooper and Jonsson, 1997). However, it is unclear whether the long positive duration in our study had any impact on CNS injury and is a component of the blast wave that will require a more thorough examination and comparison against other blast models of the same BOP but of different duration.

Separately, the blast set-up and exposure in our study also provides a platform for scaling up to other animal species and to allow comparison between species on BINT thresholds and injury presentation. In a separate study investigating effects of sub-lethal BOP on non-human primates (NHPs) in the same blast set-up, increases in TUNEL-positive cells and APP immunoreactivity in white matter, together with the darkening of neurons were also observed in NHPs exposed to 80 kPa BOP as in our rodent study (unpublished). Further investigations with different small and large animal species using the same blast set-up but with additional strain gages in the body and brains will provide useful information in how blast waves of the same pressure transmit differently through skull and brain tissue properties between species.

Our microarray studies focused on brain samples from animals exposed at the lower BOP of 48.9 kPa vs. the controls. We found 676 genes whose expression profiles were significantly altered by blast. A common feature of trauma to the CNS involves

Table 1 | Genes whose expressions show significant time-course evolution after blast in the brains of rats exposed to a BOP of 48.9 kPa.

AR	FCER1A	ITGB5	PPIB	SH3GLB1
ARHGAP4	FLT1	KIF11	PRKACB	SLC40A1
CETN1	FOLR1	KLHL10	PRKCH	TFG
COQ6	GADAY 1	MMP11	PTTG1	TPM1
CRYAB	GHR	NFKBIA	PYY	UCP1
DNAJB11	GTF2F2	PARP1	RALBP1	VEGFA
F2RL3	HMGA1	PLG	RASA3	

Table 2 | List of genes whose expression levels are significantly altered in blast-exposed animals and which also show a time-course evolution pattern between day 1, day 4, and day 7 after blast.

FLT1	GADAY 1	KIF11	PARP1	PRKCH
FOLR1	HMGA1	NFKBIA	PRKACB	SLC40A1

Table 3 | Table of illustrative examples of how genes may be classified into non-target and target groups.

Type of gene	Gene expression ratios			
	Day 1	**Day 4**	**Day 7**	**Linear/ quadratic time trend**
Gene expression is not significantly altered at any time-point and shows no time-course evolution	1.1 ($p > 0.05$)	1.1 ($p > 0.05$)	1.1 ($p > 0.05$)	$p > 0.05$
Gene expression is significantly altered by blast in some or all time points, *but* no significant time-course evolution	1.1 ($p < 0.05$) 1.1 ($p < 0.05$)	1.1 ($p < 0.05$) 1.1 ($p > 0.05$)	1.1 ($p < 0.05$) 1.1 ($p > 0.05$)	$p > 0.05$
Gene expression is not significantly altered by blast *but* overall show significant time-course evolution	1.1 ($p > 0.05$)	1.2 ($p > 0.05$)	2 ($p > 0.05$)	$p < 0.05$
Gene expression is significantly altered at least one time-point, and shows time-course evolution (overlapping genes)	1.1 ($p < 0.05$) 1.1 ($p > 0.05$)	5 ($p < 0.05$) 5 ($p < 0.05$)	1.1 ($p < 0.05$) 1.1 ($p > 0.05$)	$p < 0.05$

p-values represent the statistical significance of comparisons between blast-exposed and control samples at each time-point.

pronounced changes in the expressions of cell proliferation and apoptotic genes (Byrnes and Faden, 2007). Accordingly, we found the highest number of blast-affected genes to belong to these functional groups, suggesting that our model was fundamentally sound in approach. We also observed that the number of genes affected in all functional groups decreased from day 4 to day 7 post-blast. Based on our H&E and TUNEL observations, this corresponds to a period during which there was almost complete recovery of the brain from blast injury, suggesting that recovery from blast injury was associated with a return to baseline of the expression of most genes. However, we did not observe a similar correspondence from day 1 to day 4 post-blast, which suggests that the injury-gene expression association may be time-dependent and differ between the immediate (<day 4) and the short (day 4 to day 7) terms after blast. The difference in the expression levels at day compared to day 1 and day 7 points toward a quadratic expression profile post-blast, i.e., cluster of genes up-regulated or down-regulated at day 4 as opposed to day 1 and day 7 expression. The lack of significance may be due to the small sample size used and the result should be followed up with more extensive sampling and further analysis.

In this study, we also took a multi-pronged approach using a strategy based upon the hypothesis that any gene whose expression is significantly altered by blast exposure is more likely than any other random gene to be critically involved in blast. Likewise, genes whose expression patterns show significant time evolution following blast have higher probability than others to be functionally relevant. Note that genes in the two groups may overlap or be distinct. Based upon our strategy, it follows then that genes in the overlapping group are the more likely genes to influence clinical outcome in blast injuries. The identities of functionally relevant genes will be especially important in the design of novel therapeutics or treatment approaches in blast victims. In terms of diagnostics, however, there could be an additional level of approach besides identifying specific genes. This would involve studying the overall pattern of functional changes in gene expressions based upon the functional categorization of genes whose expressions are modulated following blast exposure. Thus, our model enables the identification of four potential markers for diagnostics and/or treatment design as summarized in **Table 3**.

We separately found 34 genes to show a time-course evolution over time after blast exposure. Ten genes were common to both our analyses (i.e., blast exposure significantly modulated their expression profiles which also changed over time). It is unclear whether

these 10 identified genes and/or their protein products critically affects injury outcome in blast victims and its reliability to form a consistent "fingerprint" of blast-induced mild TBI. Considering the 10 overlapping genes in which the involvement of some such as FLT1 (involved in cell proliferation and angiogenesis) and PARP1 (participates in DNA repair) could be said to be instinctive, that of others such as HMGA1 (commonly found in prostate tumors and thought to be involved in transformation) may be less so. It is possible that genes such as HMGA1 are also involved in injury repair which have yet to be defined. Further studies would be required to determine if this is so. However, the potential for genes and "fingerprints" identified here to be used as biomarkers and therapeutic targets in blast research cannot be denied.

Overall, we have presented a primary blast injury rodent model exposed to low BOP levels in an open-field setting. Pulmonary injury was mild and delayed whilst neuronal and non-neuronal changes were immediate at day 1 and was found to be alleviated at day 4 and day 7 suggesting the ability of the brain to recover from mild BINT on the histopathological level although it is not clear whether there is complete recovery. Acute CNS changes after low BOP exposure suggest that cortical cerebrovascular changes and white matter changes are key features of acute low level BINT. In the first, ischemia may be a resultant effect whilst predominant white matter damage suggests vulnerability to primary blast injury. Furthermore, the concomitant increases in gene expression at day 1 and day 4 suggests a time-dependent injury response and recovery period. Of the 676 genes that were significantly altered, a framework was derived to narrow these to 10 according to the time-course evolution and functional relevance. Some of these up-regulated functional genes such as FLT1 and PARP1 point toward repair after injury and may contribute to the recovery in the histopathological changes seen at day 4 and day 7. Future work will center upon the validation of our model. This would involve efforts to determine if the "fingerprints" identified here are consistent and reproducible across different animal models of blast injury and in different tissues from blast-exposed animals. Most importantly, a time-course profile of the relationship between changes in gene expression patterns, conditions of blast exposure (e.g., BOP), histopathological changes, and blast injury severity should also be evaluated and for a longer time post-blast to observe for sustained changes or the development of secondary pathobiology.

ACKNOWLEDGMENTS

The authors express their gratitude to Leonard Heng, Karen Chong, Rick Tan, Chor Boon Ng from Defence Science and Technology Agency; Julie Yeo, Jian Wu and Melissa Teo from DSO National Laboratories.

REFERENCES

Agoston, D. V., Gyorgy, A., Eidelman, O., and Pollard, H. B. (2009). Proteomic biomarkers for blast neurotrauma: targeting cerebral edema, inflammation, and neuronal death cascades. *J. Neurotrauma* 26, 901–911.

Armonda, R. A., Bell, R. S., Vo, A. H., Ling, G., DeGraba, T. J., Crandall, B., Ecklund, J., and Campbell, W. W. (2006). Wartime traumatic cerebral vasospasm: recent review of combat casualties. *Neurosurgery* 59, 1215–1225; discussion 25.

Bauman, R. A., Elsayed, N., Petras, J. M., and Widholm, J. (1997). Exposure to sublethal blast overpressure reduces the food intake and exercise performance of rats. *Toxicology* 121, 65–79.

Biomarkers Definitions Working Group. (2001). Biomarkers and surrogate endpoints: preferred definitions and conceptual framework. *Clin. Pharmacol. Ther.* 69, 89–95.

Bowen, I. G., Fletcher, E. R., and Richmond, D. R. (1968). *Estimae of Man's Tolerance to the Direct Effects of air Blast*. Albuquerque: Lovelace Foundation for Medical Education and Research.

Byrnes, K. R., and Faden, A. I. (2007). Role of cell cycle proteins in CNS injury. *Neurochem. Res.* 32, 1799–1807.

Cernak, I. (2010). The importance of systemic response in the pathobiology of blast-induced neurotrauma. *Front. Neurol.* 1:151. doi: 10.3389/fneur.2010.00151

Cernak, I., and Noble-Haeusslein, L. J. (2010). Traumatic brain injury: an overview of pathobiology with emphasis on military populations. *J. Cereb. Blood Flow Metab.* 30, 255–266.

Cernak, I., Wang, Z., Jiang, J., Bian, X., and Savic, J. (2001a). Cognitive deficits following blast injury-induced neurotrauma: possible involvement of nitric oxide. *Brain Inj.* 15, 593–612.

Cernak, I., Wang, Z., Jiang, J., Bian, X., and Savic, J. (2001b). Ultrastructural and functional characteristics of blast injury-induced neurotrauma. *J. Trauma* 50, 695–706.

Chavko, M., Prusaczyk, W. K., and McCarron, R. M. (2006). Lung injury and recovery after exposure to blast overpressure. *J. Trauma* 61, 933–942.

Chavko, M., Watanabe, T., Adeeb, S., Lankasky, J., Ahlers, S. T., and McCarron, R. M. (2011). Relationship between orientation to a blast and pressure wave propagation inside the rat brain. *J. Neurosci. Methods* 195, 61–66.

Cooper, G., and Jonsson, A. (1997). *Protection Against Blast Injury*. New York: Butterworth-Heinemann.

de Candole, C. A. (1967). Blast injury. *Can. Med. Assoc. J.* 96, 207–214.

Defense and Veterans Brain Injury Center. (2010). *Department of Defense Numbers for Traumatic Brain Injury*. Accessed January 19, 2010, from http://www.dvbic.org/TBI-Numbers.aspx

DePalma, R. G., Burris, D. G., Champion, H. R., and Hodgson, M. J. (2005). Blast injuries. *N. Engl. J. Med.* 352, 1335–1342.

Elder, G. A., Mitsis, E. M., Ahlers, S. T., and Cristian, A. (2010). Blast-induced mild traumatic brain injury. *Psychiatr. Clin. North Am.* 33, 757–781.

Fleige, S., and Pfaffl, M. W. (2006). RNA integrity and the effect on the real-time qRT-PCR performance. *Mol. Aspects Med.* 27, 126–139.

Gorbunov, N. V., Asher, L. V., Ayyagari, V., and Atkins, J. L. (2006). Inflammatory leukocytes and iron turnover in experimental hemorrhagic lung trauma. *Exp. Mol. Pathol.* 80, 11–25.

Gorbunov, N. V., McFaul, S. J., Van Albert, S., Morrissette, C., Zaucha, G. M., and Nath, J. (2004). Assessment of inflammatory response and sequestration of blood iron transferrin complexes in a rat model of lung injury resulting from exposure to low-frequency shock waves. *Crit. Care Med.* 32, 1028–1034.

Kawai, K., Nitecka, L., Ruetzler, C. A., Nagashima, G., Joo, F., Mies, G., Nowak, T. S. Jr., Saito, N., Lohr, J. M., and Klatzo, I. (1992). Global cerebral ischemia associated with cardiac arrest in the rat: I. Dynamics of early neuronal changes. *J. Cereb. Blood Flow Metab.* 12, 238–249.

Kirkman, E., and Watts, S. (2011). Characterization of the response to primary blast injury. *Philos. Trans. R. Soc. Lond., B, Biol. Sci.* 366, 286–290.

Kochanek, P. M., Bauman, R. A., Long, J. B., Dixon, C. R., and Jenkins, L. W. (2009). A critical problem begging for new insight and new therapies. *J. Neurotrauma* 26, 813–814.

Lawson Terrorism Information Centre. (2009). Terrorism incidents and significant dates calendar. Accessed May 20, 2009, from http://www.terrorisminfo.mipt.org

Ling, G., Bandak, F., Armonda, R., Grant, G., and Ecklund, J. (2009). Explosive blast neurotrauma. *J. Neurotrauma* 26, 815–825.

Long, J. B., Bentley, T. L., Wessner, K. A., Cerone, C., Sweeney, S., and Bauman, R. A. (2009). Blast

overpressure in rats: recreating a battlefield injury in the laboratory. *J. Neurotrauma* 26, 827–840.

Moochhala, S. M., Md, S., Lu, J., Teng, C. H., and Greengrass, C. (2004). Neuroprotective role of aminoguanidine in behavioral changes after blast injury. *J. Trauma* 56, 393–403.

Park, E., Gottlieb, J. J., Cheung, B., Shek, P. N., and Baker, A. J. (2010). A model of low-level primary blast exposure results in cytoskeletal proteolysis and chronic functional impairment in the brain in the absence of lung barotrauma. *J. Neurotrauma.* 28, 343–357.

Phillips, Y. Y., Mundie, T. G., Yelverton, J. T., and Richmond, D. R. (1988). Cloth ballistic vest alters response to blast. *J. Trauma* 28, S149–S152.

Rafaels, K. A., Bass, C. R., Panzer, M. B., and Salzar, R. S. (2010). Pulmonary injury risk assessment for long-duration blasts: a meta-analysis. *J. Trauma* 69, 368–374.

Readnower, R. D., Chavko, M., Adeeb, S., Conroy, M. D., Pauly, J. R., McCarron, R. M., and Sullivan, P. G. (2010). Increase in blood–brain barrier permeability, oxidative stress, and activated microglia in a rat model of blast-induced traumatic brain injury. *J. Neurosci. Res.* 88, 3530–3539.

Reneer, D. V., Hisel, R. D., Hoffman, J. M., Kryscio, R. J., Lusk, B. T., and Geddes, J. W. (2011). A multi-mode shock tube for investigation of blast-induced traumatic brain injury. *J. Neurotrauma* 28, 95–104.

Risling, M., Plantman, S., Angeria, M., Rostami, E., Bellander, B. M., Kirkegaard, M., Arborelius, U., and Davidsson, J. (2011). Mechanisms of blast induced brain injuries, experimental studies in rats. *Neuroimage* 54(Suppl. 1), S89–S97.

Saljo, A., Svensson, B., Mayorga, M., Hamberger, A., and Bolouri, H. (2009). Low-level blasts raise intracranial pressure and impair cognitive function in rats. *J. Neurotrauma* 26, 1345–1352.

Stuhmiller, J. H. (1997). Biological response to blast overpressure: a summary of modeling. *Toxicology* 121, 91–103.

Svetlov, S. I., Larner, S. F., Kirk, D. R., Atkinson, J., Hayes, R. L., and Wang, K. K. (2009). Biomarkers of blast-induced neurotrauma: profiling molecular and cellular mechanisms of blast brain injury. *J. Neurotrauma* 26, 913–921.

Svetlov, S. I., Prima, V., Kirk, D. R., Gutierrez, H., Curley, K. C., Hayes, R. L., and Wang, K. K. (2010). Morphologic and biochemical characterization of brain injury in a model of controlled blast overpressure exposure. *J. Trauma* 69, 795–804.

Treadwell, I. (1989). Effects of blasts on the human body. *Nurs. RSA* 4, 32–36.

Conflict of Interest Statement: The authors declare that the research was conducted in the absence of any commercial or financial relationships that could be construed as a potential conflict of interest.

Received: 16 February 2011; accepted: 15 March 2011; published online: 04 April 2011.

Citation: Pun PBL, Kan EM, Salim A, Li Z, Ng KC, Moochhala SM, Ling E-A, Tan MH and Lu J (2011) Low level primary blast injury in rodent brain. Front. Neur. ***2****:19. doi: 10.3389/fneur.2011.00019*

This article was submitted to Frontiers in Neurotrauma, a specialty of Frontiers in Neurology.

APPENDIX

Table A1 | Genes whose expressions are significantly altered by blast in the brains of rats exposed to a BOP of 48.9 kPa.

ABCA2	CAPZA3	DLK1	GPX3	KIF11	OMP	RAMP2	ST3GAL5
ABCC3	CASR	DNAJA3	GRIN1	KIF1C	ONECUT1	RAP1B	STAG3
ABCG2	CATSPER2	DNAJA4	GRINL1A	KIF2C	OPRL1	RAPGEF1	STC1
ABRA	CBARA1	DNAJB4	GRK1	KIT	OPRM1	RASDAY 1	STK38
ACCN2	CBR1	DNDAY 1	GRM5	KLF15	ORC2L	RASSF2	STX1A
ACHE	CCL2	DNM1L	GRPR	KLF5	OXT	RASSF5	SUFU
ACSL1	CCL3	DNMT3B	GSPT1	KLF6	P2RX2	RB1	SULT1B1
ACTB	CCL4	DPP4	GUCY1A3	KNG1	P2RY2	RBM17	SYNJ1
ADAM10	CCNB2	DPYSL5	GUSB	KRT20	PA2G4	RBP3	SYT1
ADAM9	CCNDAY 1	DR1	GZMA	LHB	PAH	RCOR2	TAAR1
ADCY6	CCNG1	DRD2	GZMB	LITAF	PAQR3	REG3G	TAC1
ADIPOR1	CCR4	DRDAY 4	H1F0	LPIN1	PARG	REST	TACC2
ADM	CCR5	DSP	HAVCR2	LPL	PARP1	RFX3	TAF5L
ADORA2A	CCT6A	DUSP5	HCLS1	LRPAP1	PARVA	RGS10	TAPBP
ADRA2B	CDAY 14	DUSP9	HCRT	LRRK2	PAX4	RGS19	TAX1BP1
AES	CD2	EBF1	HERPUDAY 1	LTB4R	PCDHAC2	RHOA	TBCE
AGRP	CD2AP	ECEL1	HES3	LTBP1	PCNA	RHOH	TBX3
AGT	CD320	ECM1	HINT1	LYPD3	PDCDAY 4	RIPK2	TCEA1
AK2	CD36	EDNRA	HIST1H1T	LZTS1	PDCD6IP	RLN1	TCIRG1
AK3L1	CD38	EGF	HIVEP1	MAEA	PDCL	RNF10	TDG
AKAP13	CD3G	EGFR	HMGA1	MAL	PDE4B	RNF14	TEAD2
AKAP4	CDAY 44	EGR1	HMMR	MAP1B	PDHA2	ROBO4	TERF1
ALB	CDC25A	EGR2	HNF4A	MAP3K10	PDLIM2	RPN2	TGFB1
ALDH2	CDC25B	EHDAY 1	HOMER1	MAPK1	PDYN	RPS15A	TGFB1I1
ALDOA	CDC2L5	EIF4B	HOMER2	MAPK14	PDZK1IP1	RRM1	TGM1
ALG5	CDC42BPB	ELA2	HOXA5	MAPK8	PELO	RTKN	TH
AMDAY 1	CDCA2	ENAH	HOXC6	MAPK9	PELP1	S100A8	THAP1
AMHR2	CDH16	ENTPDAY 1	HP	MAPRE1	PEMT	SAA4	THBD
ANTXR1	CDH22	EP400	HPS1	MAT1A	PHGDH	SATB1	THEM4
ANXA2	CDK10	ERBB2	HPSE	MATK	PIK3C3	SBDS	THPO
AOC3	CDKN1A	ESM1	HSDAY 11B2	MATR3	PIR	SCAMP2	TIAM1
APBA1	CDKN1B	ETS2	HSPA1A	MBL2	PKDAY 1	SCARB1	TK1
APCS	CDKN1C	ETV6	HSPA8	MCF2L	PKNOX1	SCN10A	TLE4
APH1A	CDX2	F12	HSPBP1	MFN2	PLA2G4A	SCN4B	TMOD2
APH1B	CEBPE	F2R	HSPDAY 1	MGAT2	PLAT	SCN9A	TMOD3
APLN	CES1	F2RL2	HTR1B	MINA	PLCG1	SCNN1B	TNF
APOC2	CFH	F5	HTR1D	MLH1	PLD2	SEMA3D	TNFRSF1A
AQP4	CFTR	FABP7	HTR2A	MLL	PLEKHF1	SENP2	TNNI2
AREG	CGA	FADS1	HTR2B	MST1	PLXNA3	SERINC3	TNNT1
ARF6	CHI3L1	FAIM	IBSP	MSX2	PMCH	SERPINB2	TNP2
ARHGEF7	CHMP5	FAU	ICAM1	MTA1	PNLIP	SERPINI1	TNR
ARL11	CHRM4	FCGR3A	ID2	MTPN	POLA1	SFRP2	TOB2
ARL2BP	CHRNA10	FGF13	ID3	MXD3	PON2	SFRS2	TOP2A
ASAH2	CIT	FGF4	IFNG	MXI1	POU2F1	SFTPC	TPH1
ATF3	CITED2	FGFR1	IGF1R	MYCL1	POU2F2	SGTB	TPM3
ATG7	CKAP5	FGG	IGFBP1	MYO5A	POU3F1	SH3BP5	TPST1
ATP1A1	CLDN11	FGL2	IGFBP4	NAP1L1	PPAP2C	SHC1	TPT1
ATP2A3	CLU	FGR	IGHMBP2	NCR3	PPEF1	SHH	TRADD
ATP2C2	CNR1	FHIT	IKBKG	NDFIP1	PPIL2	SHMT1	TRIB3

(Continued)

Table A1 | Continued

ABCA2	CAPZA3	DLK1	GPX3	KIF11	OMP	RAMP2	ST3GAL5
ATP6V1C1	CNTF	FKRP	IL12RB2	NDN	PPM1J	SIP1	TRIM32
ATP6V1F	CNTN3	FLT1	IL13	NDRG1	PPP1R1B	SIX3	TRIM63
ATP7B	CNTN4	FN1	IL13RA1	NEFL	PPP2R2B	SLC16A2	TRPC3
AVP	COL16A1	FOLR1	IL13RA2	NEO1	PPP2R3A	SLC16A4	TRPM6
AZGP1	COL2A1	FOXM1	IL18RAP	NEU1	PPP2R5B	SLC17A3	TRPM7
AZI2	COMT	FSHR	IL1A	NEU3	PPYR1	SLC18A2	TRPV1
B4GALNT1	CORO1B	FTH1	IL1B	NEUROG3	PRDX5	SLC1A3	TTN
BACE1	CREB1	FUBP1	IL22RA2	NFIA	PRIM1	SLC22A2	TTR
BAD	CRKRS	FUT4	IL4	NFKBIA	PRKAB1	SLC24A3	TUBB2C
BAK1	CRTC2	FXYD5	IL8RB	NFKBIB	PRKACB	SLC25A10	TWIST1
BCAN	CRY1	GABBR1	IMPACT	NGFR	PRKCD	SLC25A14	UBC
BCAP31	CSDA	GADAY 1	IMPDH2	NIDAY 1	PRKCH	SLC25A27	UBE2D2
BCL2	CSF3	GADDAY 45GIP1	INHBB	NINJ2	PRKCZ	SLC2A4	UBE2D3
BCL2L10	CSNK1A1	GALNS	INSIG2	NKX3-1	PRLR	SLC34A1	UBTF
BDKRB2	CSNK1G1	GAP43	INSRR	NLGN3	PRM1	SLC36A2	UCHL1
BID	CSPG4	GATA1	IPPK	NMT1	PRPF19	SLC37A4	UCP2
BMP4	CSPG5	GATA6	IRS1	NNT	PRPF8	SLC40A1	UGCG
BNIP3	CTH	GATAD2A	ITGA1	NOS3	PSMB2	SLC6A3	USH2A
BTRC	CTNNB1	GFAP	ITGA2	NOVA1	PSMD2	SLC6A4	USP14
BYSL	CTSB	GGCX	ITGA4	NPDC1	PSMDAY 4	SLC6A5	VNN1
C3AR1	CUGBP1	GHRL	ITGA5	NPEPPS	PSMD9	SLC7A2	VPS4B
C9	CXCL11	GLI1	ITGAL	NPFF	PTGDS	SLC7A5	VTCN1
CA3	CYB5R4	GLIPR1	ITGB2	NPR1	PTGER4	SLC8A1	WEE1
CABP1	CYP1A1	GLP2R	ITPKB	NPY	PTGES	SLC9A1	WNT2
CACNA1B	CYP2E1	GLTSCR2	JAG1	NR1D2	PTGS2	SMAD3	XRCC1
CACNB2	CYR61	GNA14	JAM2	NR1I2	PTHLH	SMO	YBX1
CALCA	DAB2	GNAL	KCNA1	NR2C2	PTK2	SNAPC2	ZBTB10
CALCRL	DBH	GNB2	KCNA6	NR2F2	PTMS	SNCA	ZDHHC2
CALDAY 1	DCC	GNB5	KCNC1	NR4A3	PTPN2	SOD3	ZHX2
CAMK2A	DCLK1	GNG2	KCNC3	NR5A2	PTPN3	SP2	ZIC1
CAMK4	DDR1	GNG4	KCNH1	NRTN	PTPRV	SPG7	ZMYNDAY 11
CAMKK1	DEAF1	GNG5	KCNJ11	NRXN2	PTS	SPP1	ZP2
CAMKK2	DGAT1	GNRH1	KCNMA1	NTRK1	QPRT	SQSTM1	
CAMP	DGAT2	GPC1	KCNMB1	NTRK2	RABGGTA	SREBF2	
CANT1	DKC1	GPR44	KCNN3	NUP98	RAG1	SST	
CAPN2	DLC1	GPS1	KIDINS220	OMG	RALGDS	ST18	

Table A2 | Biological functions of genes in each cluster (clusters 1–4, 6, and 7; except clusters 5 and 8 which do not have genes with information).

Category	Molecules
CLUSTER 1 FUNCTIONS	
Amino acid metabolism	GADAY 1
Antigen presentation	PLG, NFKBIA, VEGFA, ITGB5
Carbohydrate metabolism	GPI, F2RL3
Cell cycle	PLG, CETN1, NFKBIA, VEGFA, KIF11, CLIP1, GPI, CRYAB, GHR
Apoptosis	LPAR1, NFKBIA, VEGFA
Cell morphology	PLG, LPAR1, NFKBIA, VEGFA, CLIP1, ITGB5, GPI, GHR
Cell signaling	PLG, LPAR1, VEGFA, FCER1A, PYY, ARHGAP4, PPIB, F2RL3
Cell-to-cell signaling and interaction	PLG, VEGFA, PRKACB, PYY, ITGB5, GPI, GHR
Cellular assembly and organization	CETN1, LPAR1, SH3GLB1, VEGFA, FCER1A, ITGB5, F2RL3, CRYAB, PLG, KIF11, CLIP1, ARHGAP4, GPI, GHR
Cellular compromise	PLG, VEGFA, KIF11, GPI, GHR
Cellular development	PLG, NFKBIA, VEGFA, FCER1A, GHR
Cellular function and maintenance	PLG, NFKBIA, KIF11, PYY, ITGB5, ARHGAP4, GPI, F2RL3, GHR
Cellular growth and proliferation	LPAR1, VEGFA, C19ORF10, ITGB5, PYY,CRYAB, PLG, TFG, NFKBIA, KIF11, GADAY 1, GPI, WNK1, GHR, SKAP2
Cellular movement	PLG, LPAR1, NFKBIA, VEGFA, PYY, ITGB5, GADAY 1, GPI, PPIB
DNA replication, recombination, and repair	VEGFA, PPIB, WNK1, GHR
Drug metabolism	VEGFA, PPIB, GHR
Energy production	PLG
Gene expression	NFKBIA, VEGFA, GHR
Lipid metabolism	NFKBIA, VEGFA, PYY, GHR
Molecular transport	PLG, LPAR1, NFKBIA, VEGFA, FCER1A, PYY, GPI, PPIB, F2RL3, GHR
Nucleic acid metabolism	PLG, VEGFA, PPIB, WNK1, GHR
Post-translational modification	VEGFA, GADAY 1
Protein folding	VEGFA
Protein synthesis	PLG, VEGFA, PYY
Protein trafficking	NFKBIA
Small molecule biochemistry	PLG, NFKBIA, VEGFA, PYY, GADAY 1, GPI, PPIB, F2RL3, WNK1, GHR
Vitamin and mineral metabolism	PLG, LPAR1, VEGFA, FCER1A, PYY, PPIB, F2RL3
Immune response	PLG, VEGFA, FCER1A, ITGB5
CLUSTER 2 FUNCTIONS	
Amino acid metabolism	HIPK2, PRKCH, PPM1D
Antigen presentation	PPM1D
Carbohydrate metabolism	UCP1
Cell cycle	HIPK2, PRKCH, PPM1D
Apoptosis	HIPK2
Cell morphology	PRKCH, UCP1
Cell signaling	HIPK2
Cellular assembly and organization	HIPK2
Cellular compromise	HIPK2, UCP1
Cellular development	HIPK2, PRKCH
Cellular function and maintenance	UCP1, PPM1D
Cellular growth and proliferation	HIPK2, PRKCH, UCP1
DNA replication, recombination, and repair	PRKCH, UCP1
Drug metabolism	UCP1
Energy production	UCP1
Free radical scavenging	UCP1
Gene expression	PRKCH, UCP1
Lipid metabolism	UCP1
Molecular transport	PRKCH, UCP1
Nucleic acid metabolism	UCP1
Post-translational modification	HIPK2, PRKCH, PPM1D
Small molecule biochemistry	HIPK2, PRKCH, UCP1, PPM1D
Immnue response	PPM1D
CLUSTER 3 FUNCTIONS	
Amino acid metabolism	PARP1
Antigen presentation	FLT1, IRF8
Carbohydrate metabolism	PARP1, FLT1, RALBP1
Cell cycle	DDB1, PARP1, FLT1, TPM1, HMGA1
Apoptosis	PARP1, NDRG1, FLT1, RALBP1, TPM1, COQ6, HMGA1, IRF8
Cell morphology	FLT1, CDAY 151, RALBP1, TPM1, HMGA1
Cell signaling	FLT1
Cell-to-cell signaling and interaction	FLT1, CDAY 151, IRF8
Cellular assembly and organization	PARP1, FLT1, TPM1
Cellular compromise	KLHL10, PARP1, NDRG1, FLT1, TPM1, HMGA1
Cellular development	KLHL10, PARP1, NDRG1, FLT1, VSX2, CDAY 151, RALBP1, TPM1, HMGA1, RASA3, IRF8
Cellular function and maintenance	PARP1, FLT1, TPM1, IRF8
Cellular growth and proliferation	NDRG1, FLT1, VSX2, RALBP1, TPM1, HMGA1, IRF8
Cellular movement	PARP1, FLT1, CDAY 151, RALBP1, TPM1

(Continued)

Table A2 | Continued

Category	Molecules
Cellular response to therapeutics	PARP1
DNA replication, recombination, and repair	DDB1, PARP1, HMGA1
Drug metabolism	PARP1, RALBP1
Energy production	PARP1
Gene expression	DDB1, PARP1, GTF2F2, VSX2, RALBP1, HMGA1, IRF8
Lipid metabolism	FDPS, FLT1
Molecular transport	PARP1, RALBP1
Nucleic acid metabolism	DDB1, PARP1, RALBP1
Post-translational modification	PARP1
RNA post-transcriptional modification	PARP1
Small molecule biochemistry	DDB1, FDPS, PARP1, FLT1, RALBP1
Immune response	FLT1, IRF8
CLUSTER 4 FUNCTIONS	
Amino acid metabolism	FOLR1
Antigen presentation	MMP11
Carbohydrate metabolism	INPP5K
Apoptosis	MMP11
Cellular assembly and organization	INPP5K
Cellular function and maintenance	FOLR1, SLC40A1
Cellular growth and proliferation	MMP11, FOLR1
DNA replication, recombination, and repair	FOLR1
Drug metabolism	FOLR1
Lipid metabolism	INPP5K
Molecular transport	INPP5K, FOLR1, SLC40A1
Nucleic acid metabolism	FOLR1
Post-translational modification	MMP11
Protein synthesis	FOLR1
Protein trafficking	FOLR1
Small molecule biochemistry	INPP5K, FOLR1, SLC40A1
Vitamin and mineral metabolism	FOLR1
Immune response	MMP11
CLUSTER 6 FUNCTIONS	
Cellular assembly and organization	EIF4A1
Gene expression	EIF4A1
Protein synthesis	EIF4A1
RNA post-transcriptional modification	EIF4A1
RNA trafficking	EIF4A1
CLUSTER 7 FUNCTIONS	
Carbohydrate metabolism	PTTG1
Cell cycle	AR, PTTG1
Apoptosis	AR, PTTG1
Cell morphology	AR, PTTG1
Cell signaling	AR
Cell-to-cell signaling and interaction	AR
Cellular assembly and organization	AR, PTTG1
Cellular compromise	AR, PTTG1
Cellular development	AR, PTTG1
Cellular function and maintenance	AR
Cellular growth and proliferation	AR, PTTG1
Cellular movement	AR
DNA replication, recombination, and repair	AR, PTTG1
Drug metabolism	AR, PTTG1
Gene expression	AR, PTTG1
Lipid metabolism	AR, PTTG1
Molecular transport	AR, PTTG1
Nucleic acid metabolism	AR
RNA damage and repair	DNAJB11
RNA post-transcriptional modification	DNAJB11
Small molecule biochemistry	AR, PTTG1
Immune response	AR, PTTG1